Electronic Supplementary Material (ESI) for Journal of Materials Chemistry A.

Supporting Information

Room-Temperature-Processing Fullerene Single-Crystalline Nanoparticles for High-Performance Flexible Perovskite Photovoltaics

Xiaoming Zhao[1,4,5,#], *Lixian Tian*[2,4], *Tianjun Liu*[3,5], *Hongli Liu*[1,4,*], *Shirong Wang*[1,4,*], *Xianggao Li*[1,4], *Oliver Fenwick*[3,5], *Shengbin Lei*[2,4] *and Wenping Hu*[2,4]

1 School of Chemical Engineering and Technology, Tianjin University, Tianjin 300354, China.

2 Department of Chemistry, Tianjin Key Laboratory of Molecular Optoelectronic Science, School of Science, Tianjin University, Tianjin 300072, China

3 School of Engineering and Materials Science, Queen Mary University of London, 327 Mile End Road, London E1 4NS, United Kingdom.

4 Collaborative Innovation Center of Chemical Science and Engineering (Tianjin), Tianjin 300072, China.

5 Materials Research Institute, Queen Mary University of London, 327 Mile End Road, London E1 4NS, United Kingdom

*Corresponding Authors: liuhongli@tju.edu.cn (Hongli Liu); wangshirong@tju.edu.cn (Shirong Wang)

Present Address: Department of Chemical and Biological Engineering, Princeton University, Princeton, New Jersey 08544, United States

Keywords: fullerene nanoparticles; single crystal; organic scaffold; perovskite solar cells.

Experimental Section

Materials: FTO glass (<15 Ω/square) and ITO glass (<10 Ω/square) were purchased from Advanced Election Technology Co., Ltd. ITO-coated polyethylene-naphthalate (PEN) substrates (<15 Ω/square) were purchased from Diamond Coatings Ltd. 2,2,',7,7'-tetrakis-(N,N-di-p-methoxyphenyl-amine)-9,9-spirobifluorene (spiro-OMeTAD), lithium bis(trifluoromethanesulfonyl)imide (Li-TFSI), 4-tert-butylpyridine (*t*-BP), CH_3NH_3I (MAI) and PbI_2 were purchased from Advanced Election Technology Co., Ltd. C_{60} with purity of 99.5% was purchased from Ossila Co., Ltd. Titanium diisopropoxide bis(acetylacetonate) was purchased from Alfar Aesar. N-butanol, acetonitrile, ethonal and other solvents were purchased from Shanghai Aladdin Biochemical Technology Co., Ltd. All the materials were used as received without any other purification unless otherwise specified.

Preparation of C_{60}-NPs: The preparation of C_{60} nanoparticles was carried out following the previous report.[1] Typically, C_{60} powder (3 mg) was was dissolved in 1 mL of HPLC-grade toluene by stirring for a few hours, resulting in a clear dark purple solution. This solution was then gently injected into a 20 mL of strongly stirring ethnol. The mixture was sonicated with a sonicating probe in a fume hood for more than 24 h to allow for the evaporation of toluene and ethanol. Throughout this sonication process, the mixture was topped off with ethanol every 1 hour to compensate for solvent loss through evaporation. The final solution was filtered, first through a 0.45 μm membrane filter followed by a 0.2 μm membrane filter and a stock dispersion was obtained readily for device fabrication. The concentration of C_{60}-NPs can be adjusted through the evaporation of ethonal. The whole preparation wes conducted in ambient condition at room temperature.

Characterization and Crystallography: SEM images were recorded by an FEI Inspect-F scanning electron microscope. Bruker Dimension ICON atomic force microscope in tapping mode was used to characterize surface morphology of the C_{60}-NPs. TEM observations were performed with an ED configuration on a JEOL JEM-2010 transmission electron microscope with an accelerating voltage of 200 kV. X-ray diffraction (XRD) data was recorded on the Mini Flex 600 using CuKα radiation. Time-resolved photoluminescence (TRPL) spectra and steady-state photoluminescence was recorded on Edinburgh Instruments Photoluminescence Spectrometer (FLS 980, UK) collected at 780 nm and excitation at 465 nm. The transmittance and absportion of the substrate with different ETLs was investigated by UV-Vis spectrometer (Cary 5000, Agilent technologies) in the visible range from 300 to 800 nm. Electrochemical impedance spectroscopy (EIS) was performed using an electrochemical workstation (Vertex. One. EIS, Ivium) under dark and a frequency ranging from 1 MHz to 100 mHz was applied. The IPCE of the devices was measured by focusing light from a 300W Xenon lamp (ILC Technology, USA) through a Gemini-180 double monochromator (Jobin Yvon Ltd., UK). The space charge limited current (SCLC) measurement were performed through Keithley source table (Keithley 2400,USA). The *J-V* characteristics of the devices were measured under 100 mW cm^{-2} conditions using a 450 W Xenon lamp (Oriel), as a light source, equipped with a Schott K113 Tempax sunlight filter (Praezisions Glas & Optik GmbH) to match the emission spectra to the AM1.5G standard in the region of 350-750 nm. The *J-V* curves of all devices were measured by masking the active area with a metal mask of area 0.05 cm^2 without any preconditioning of the solar cells with scan speed and dwell time of 0.125 V s^{-1} and 0.05 s, respectively.

Fabrication of PSCs based on c-TiO_2/m-TiO_2 ETLs: FTO-coated glass substrates were washed for 15 min sequentially in detergent, toluene, deionized water and ethanol. Immediately after the cleaning, the FTO substrates are transferred to a hot plate and quickly warmed up to 450 ºC (within 30 min). The substrates are left for 15 min at 450ºC before depositing the compact TiO_2 layer by aerosol spray pyrolysi. A compact TiO_2 layer was deposited by spray pyrolysis of 7 ml 2-propanol solution containing 0.6 mL titanium diisopropoxide bis(acetylacetonate) solution (75% in 2-propanol, Sigma-Aldrich) and 0.4 mL acetylacetone at 450 °C in air. After cooling to RT, on top of this layer, mesoporous TiO_2 was made by spin-coating 30 nm sized commercial TiO_2 paste (Dyesol 30NRD, Dyesol) diluted in ethanol (1:5.5 w/w) at 4500 rpm for 20 s with 2000 rpm/s acceleration rate. Immediately after the spinning, the layer is dried at 70 ºC for a few minutes. Subsequently, the substrate was sintering at 500 °C for 30 min in air. The $CH_3NH_3PbI_3$ layer was fabricated by one step fast crystallization method and the precursor solution was prepared from 1.35M Pb^{2+} dissolved in DMF and DMSO (the volume ratio of DMF/DMSO is 4:1). The spin-coating procedure was performed at 2000 rpm (acceleration rate 200 rmp/s) for 10 s and 6000 rpm (accelaration rate 1000 rmp/s) for 30 s. Diethyl ether (500 μL) was dropped in the spin-coating step 21 s before the end of the procedure in glovebox. The perovskite film was then heated at 100 °C for

60 min on a hotplate. Subsequently, the spiro-OMeTAD was deposited on top of the perovskite by spin-coating at 4000 rpm (acceleration rate 2000 rmp/s) for 20 s. The spiro-OMeTAD solutions were prepared by dissolving spiro-OMeTAD in chlorobenzene (1 mL) at a concentration of 72.3 mg mL^{-1} with the addition of 30 μL TBP and 18 μL acetonitrile solution of 520 mg/mL Li-TFSI in glovebox. And devices were finalized by the thermal evaporation of 80 nm gold.

Fabrication of PSCs based on c-C_{60}/C_{60}-NPs ETLs: The commercially purchased ITO -coated glass substrate was used after sequential cleaning by ultrasonic method with acetone, isopropanol, and DI water. After drying with nitrogen gas, the ITO glass substrate was exposed to UVO treatment in order to improve the surface energy. 10 nm compact C_{60} films were thermally depostited on the ITO glass substrate at a rate of ~0.1 A s^{-1} by thermal evaporator in a vacuum condition under < 10^{-7} Torr. The deposition rate and thickness of the organic layer were controlled by a quartz crystal sensor during the thermal evaporation process. In the optimized procedure, organic scaffold with a thinkness of 50 nm was prepared by spin-coating as-prepared C_{60}-NPs onto C_{60} compact layer at 4000 rpm (acceleration rate 2000 rmp/s) for 60 s and then put the substrate into a vacuum oven with a temperature of 25℃ under a background pressure of 10^{-5} Torr to remove the remaining solvents. $CH_3NH_3PbI_3$ layer was fabricated by one step fast crystallization method and the precursor solution was prepared from 1.35M Pb^{2+} dissolved in DMF and DMSO (the volume ratio of DMF/DMSO is 4:1). The spin-coating procedure was performed at 2000 rpm (acceleration rate 200 rmp/s) for 10 s and 6000 rpm (acceleration rate 2000 rmp/s) for 30 s. Diethyl ether (500 μL) was dropped in the spin-coating step 25 s before the end of the procedure in glovebox. The perovskite film was then heated at 100 ℃ for 60 min on a hotplate. Subsequently, the spiro-OMeTAD was deposited on top of the perovskite by spin-coating at 4000 rpm (acceleration rate 2000 rmp/s) for 20 s. The Spiro-OMeTAD solutions were prepared by dissolving spiro-OMeTAD in chlorobenzene (1 mL) at a concentration of 72.3 mg/mL with the addition of 30 μL TBP and 18 μL acetonitrile solution of 520 mg/mL Li-TFSI in glovebox. And devices were finalized by the thermal evaporation of 80 nm gold. Flexible perovskite solar cells comprised of PEN/ITO/c-C_{60}/C_{60}-NPs/$MAPbI_3$/HTM/Au structures were also fabricated. The c-C_{60}/C_{60}-NPs ETL was deposited on the ITO-coated PEN substrate using the same procedure described above. Other layers were sequentially deposited by using the same procedure described above.

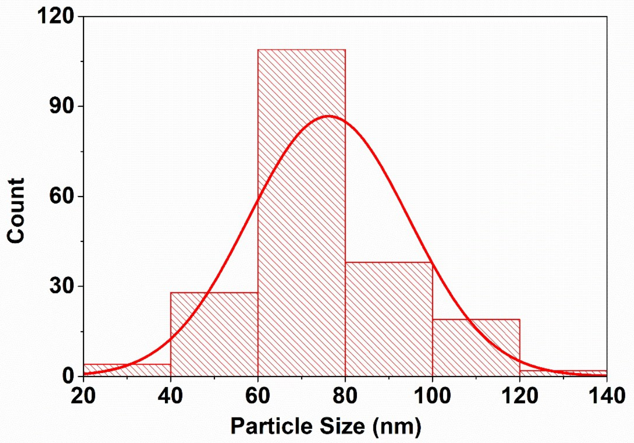

Figure S1 Distribution curve of C_{60}-NPs.

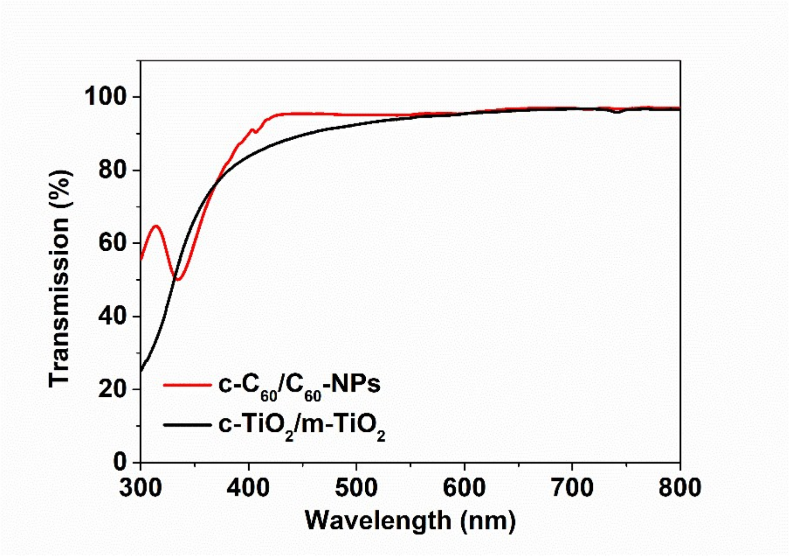

Figure S2 Transmission spectrum of c-TiO_2/m-TiO_2 and c-C_{60}/C_{60}-NPs films deposited on a glass substrate.

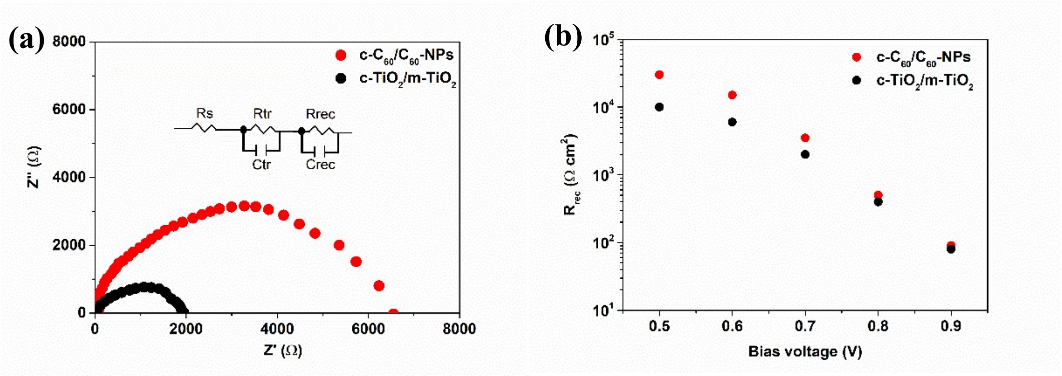

Figure S3 Nyquist plots of (a) the EIS of the PSCs based on c-TiO_2/m-TiO_2 and c-C_{60}/C_{60}-NPs at 0.7 V in the dark and (b) the R_{rec} of the PSCs based c-TiO_2/m-TiO_2 and c-C_{60}/C_{60}-NPs at different bias voltages, respectively.

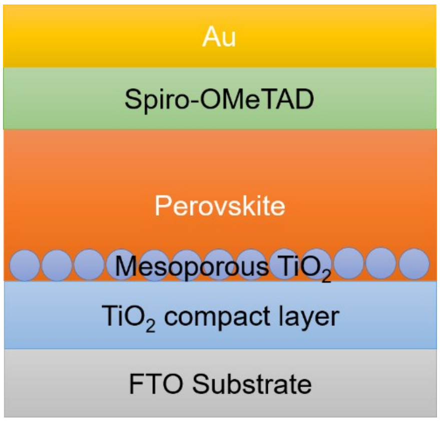

Figure S4 The structures of conventional perovskite solar cells with mesoporous TiO_2 and compact TiO_2 as an ETL.

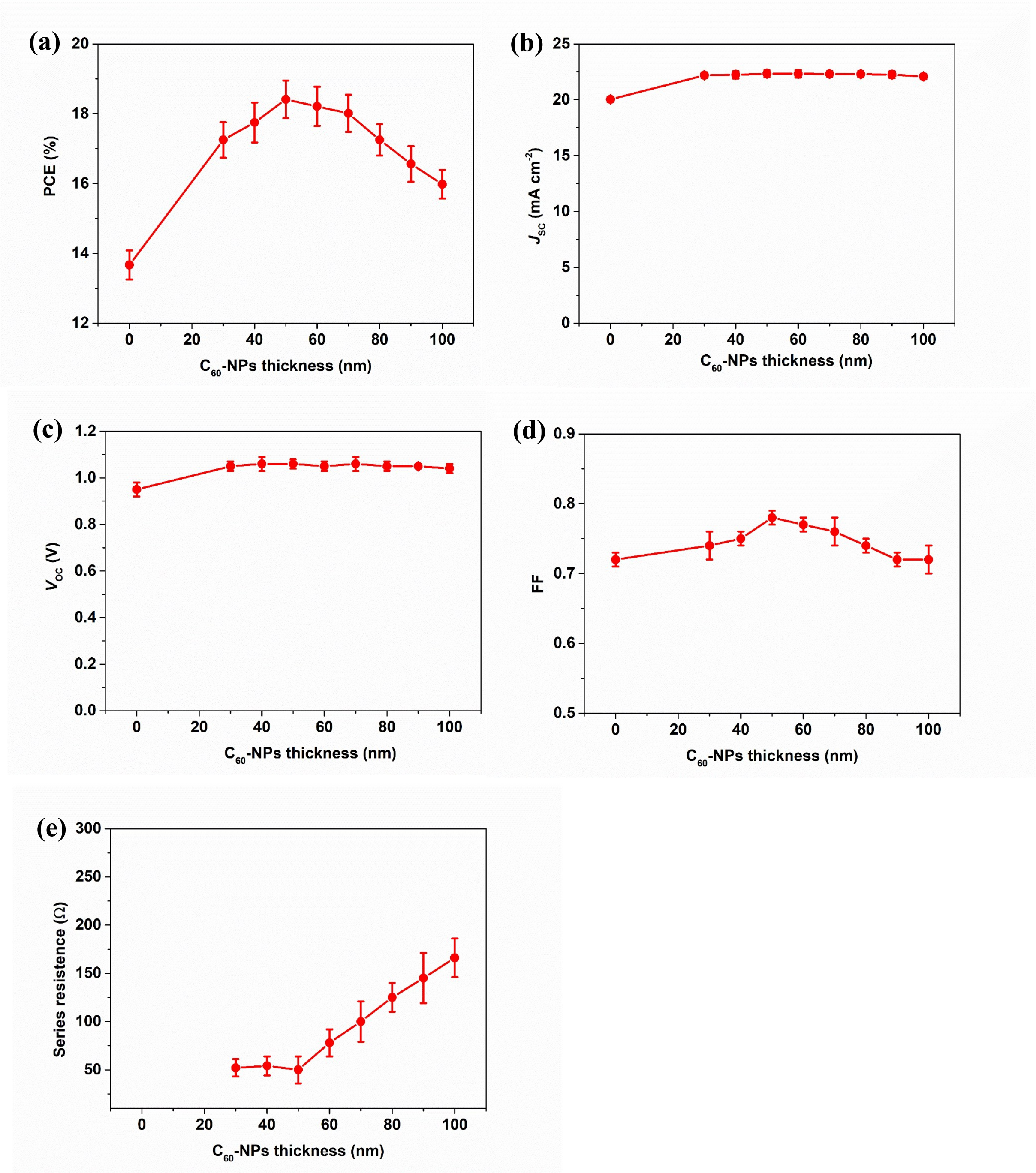

Figure S5 Dependence of (a) PCE, (b) short-circuit photocurrent density, (c) open-circuit voltage, (d) fill factor and (e) series resistance on C_{60}-NPs thickness in $MAPbI_3$ OPSCs with c-C_{60}/C_{60}-NPs ETLs measured under one-sun illumination in reverse voltage scan.

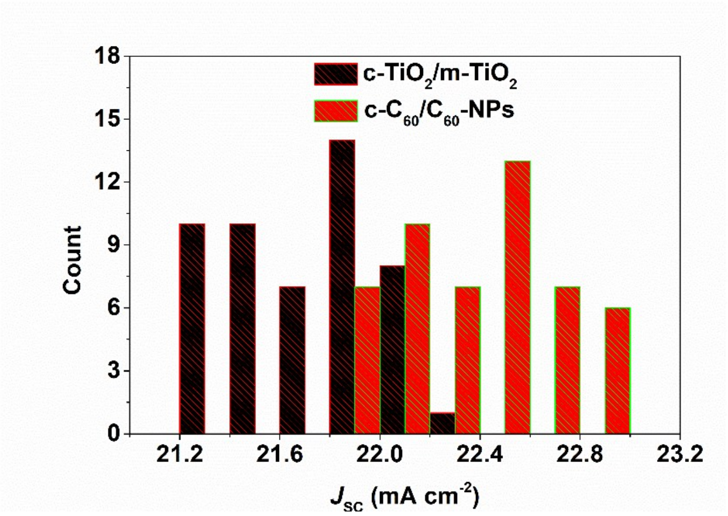

Figure S6 J_{SC} metrics of devices based on corresponding ELTs in reverse scan.

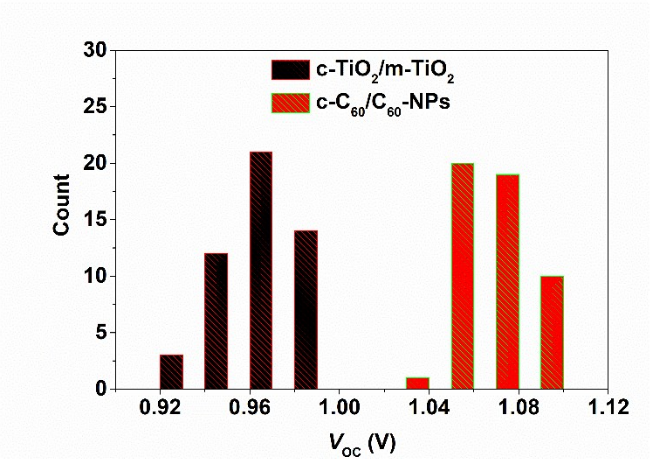

Figure S7 V_{OC} metrics of devices based on corresponding ELTs in reverse scan.

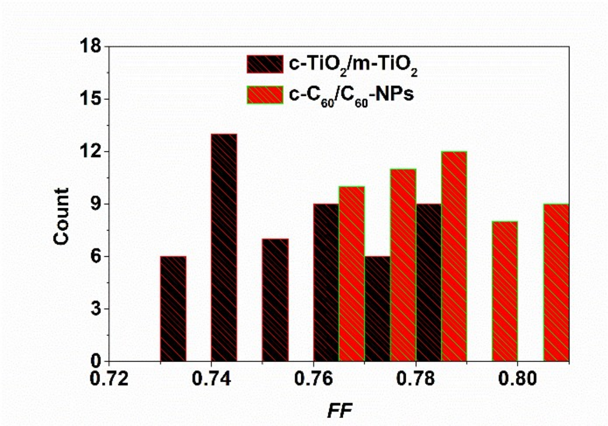

Figure S8 *FF* metrics of devices based on corresponding ELTs in reverse scan.

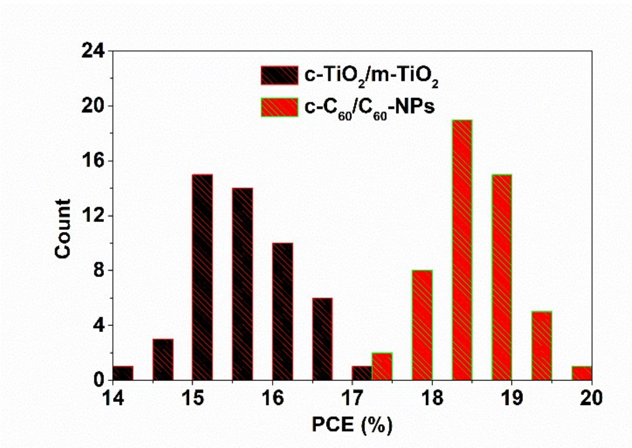

Figure S9 PCE metrics of devices based on corresponding ELTs in reverse scan.

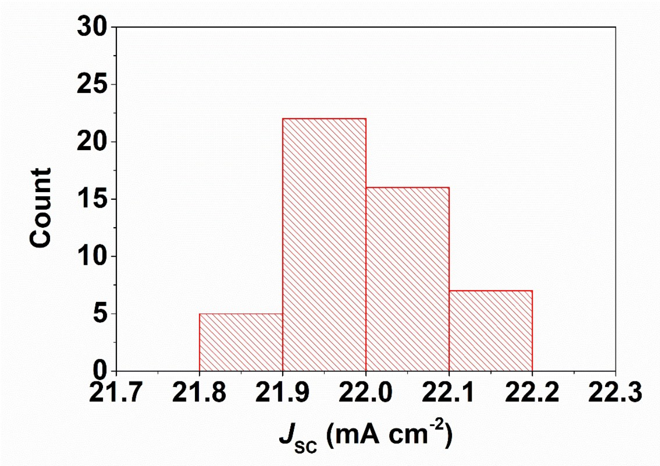

Figure S10 J_{SC} metrics of flexible devices.

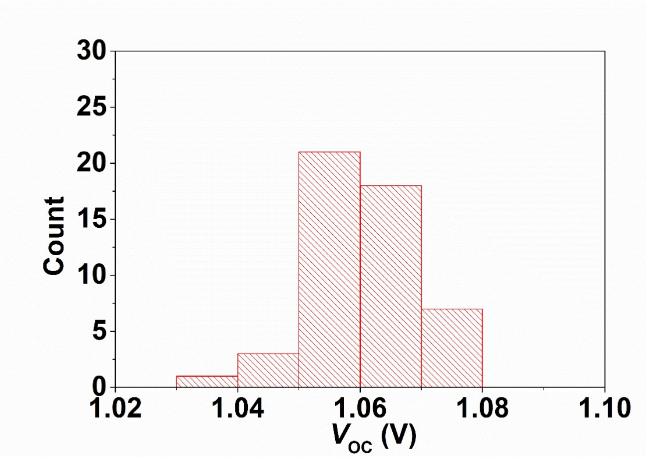

Figure S11 V_{OC} metrics of flexible devices.

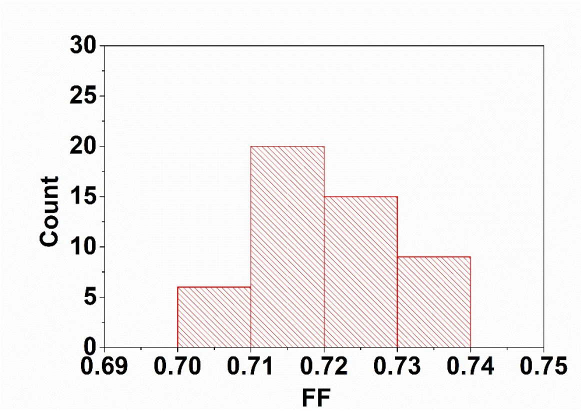

Figure S12 *FF* metrics of flexible devices.

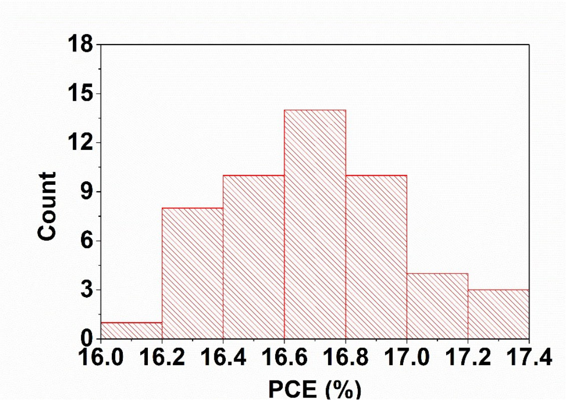

Figure S13 PCE metrics of flexible devices.

Reference

1 G. V. Andrievsky, M. V. Kosevich, O. M. Vovk, V. S. Shelkovsky and L. A. Vashchenko, *J. Chem. Soc. Chem. Commun.*, 1995, 1281–1282.